Available online at www.sciencedirect.com
ScienceDirect
Journal of Power Sources 160 (2006) 1342–1348
JOURNAL OF POWER SOURCES
www.elsevier.com/locate/jpowsour

# Preparation and electrochemical characteristics of $LiNi_{1/3}Mn_{1/3}Co_{1/3}O_2$ coated with metal oxides coating

Decheng Li [a], Yasuhiro Kato [b], Koichi Kobayakawa [b], Hideyuki Noguchi [c], Yuichi Sato [b,*]

[a] *High-Tech Research Center, Kanagawa University, 1-1-40 Suehiromachi, Tsurumi-ku,Yokohama 230-0045, Japan*
[b] *Department of Applied Chemistry, Kanagawa University, 3-27-1 Rokkakubashi, Kanagawa-ku, Yokohama 221-8686, Japan*
[c] *Department of Applied Chemistry, Saga University, Honjyo-1, Saga 840-8502, Japan*

Received 20 December 2005; received in revised form 13 February 2006; accepted 15 February 2006
Available online 18 April 2006

**Abstract**

$LiNi_{1/3}Mn_{1/3}Co_{1/3}O_2$ prepared by a spray drying method exhibited poor cyclic performance when it was operated at rates of 0.5*C* and 2*C* in 3–4.6 V. A metal oxide ($ZrO_2$, $TiO_2$, and $Al_2O_3$) coating (3 wt%) could effectively improve its cyclic performance at both 0.5*C* and 2*C*. Electrochemical impedance spectroscopy (EIS) studies suggested that both the surface resistance and the charge transfer resistance of the bare $LiNi_{1/3}Mn_{1/3}Co_{1/3}O_2$ significantly increase after 100 cycles, whose origin is mainly related to the change in both the particle surface and electrode morphologies. The presence of a thin metal oxide layer could remarkably suppress the increase in the total resistance (sum of the surface resistance and the charge transfer resistance), which was attributed to the improvement in good cyclic performances.


*Keywords:* Lithium ion battery; Cathode material; $LiNi_{1/3}Mn_{1/3}Co_{1/3}O_2$; Metal oxides coating; Improved cyclic performance

## 1. Introduction

A layered compound, $LiNi_{1/3}Mn_{1/3}Co_{1/3}O_2$, which was first proposed by Ohzuku and Makimura [1], has been extensively studied as a promising cathode material for lithium ion batteries [2–10]. It has many advantages over other candidates, such as a high discharge capacity, high rate capability, and good structural stability. A close inspection of the published literature reveals that its cyclic performance in the high voltage range (for example, 3–4.6 V) seems to be unsatisfactory [2,3,5], the mechanism of which has not been completely clarified [11,12]. It has been reported that a fluorine-substituted $LiNi_{1/3}Mn_{1/3}Co_{1/3}O_2$ would exhibit an improved cycleability in the 3–4.6 V range [10,11,13]. Our recent study suggested that the capacity fading was related to both the operating current density and cutoff voltage, and the unstable surface layer between the active particles and the electrolyte solution contributed to the cycling deterioration [14]. It is well-known that a metal oxide coating could significantly upgrade the cyclic characteristics of the cathode materials although its mechanism is still a controversial issue [15–17]. Nevertheless, the electrochemical properties of the $LiNi_{1/3}Mn_{1/3}Co_{1/3}O_2$ with a metal oxide coating are seldom reported. Thus, it is necessary to study the influence of the metal oxide coating on the electrochemical properties of the $LiNi_{1/3}Mn_{1/3}Co_{1/3}O_2$, which is meaningful and helpful to elucidate the mechanism of the cyclic fading at high voltage.

In this study, $LiNi_{1/3}Mn_{1/3}Co_{1/3}O_2$ with a metal oxide coating ($ZrO_2$, $TiO_2$, and $Al_2O_3$) was prepared, and improved high voltage cyclic performances at relatively high current densities were observed.

## 2. Experimental

### 2.1. Preparation of $LiNi_{1/3}Mn_{1/3}Co_{1/3}O_2$

The $LiNi_{1/3}Mn_{1/3}Co_{1/3}O_2$ used in this study was prepared by a spray drying method. Generally, stoichiometric starting materials, $Ni(CH_3COO)_2{\cdot}4H_2O$, $Mn(CH_3COO)_2{\cdot}4H_2O$, $Co(CH_3COO)_2{\cdot}4H_2O$, and $LiNO_3$, were initially dissolved in distilled water to obtain a solution. The resulting solution was pumped into a spray drying instrument (Büchi Mini Spray Dryer B-290). The obtained precursor was pre-heated at 400 °C. After being ground and pressed into pellets, it was sintered at 900 °C for 15 h in air.

* Corresponding author. Tel.: +81 45 481 5661x3885; fax: +81 45 413 9770.
*E-mail address:* satouy01@kanagawa-u.ac.jp (Y. Sato).

0378-7753/$ – see front matter © 2006 Elsevier B.V. All rights reserved.
doi:10.1016/j.jpowsour.2006.02.080

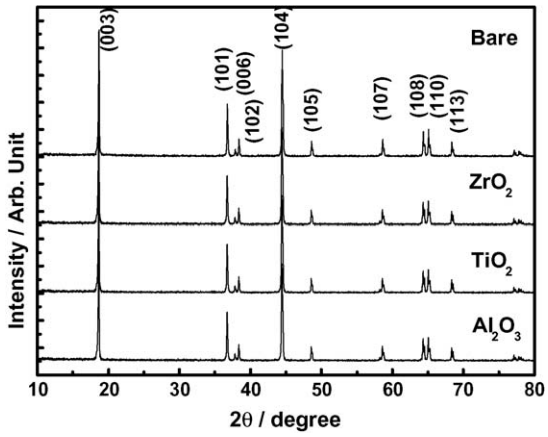


Fig. 1. XRD profiles of the bare $LiNi_{1/3}Mn_{1/3}Co_{1/3}O_2$ and $LiNi_{1/3}Mn_{1/3}Co_{1/3}O_2$ coated with the metal oxides.

### 2.2. Preparation of $LiNi_{1/3}Mn_{1/3}Co_{1/3}O_2$ coated with metal oxides

$Zr[O(CH_2)_3CH_3]_4$, $Ti[O(CH_2)_3CH_3]_4$, and $Al(C_3H_7O)_3$ were each initially dissolved in ethyl alcohol, respectively, and dispersed by an ultrasonic cleaner. The obtained $LiNi_{1/3}Mn_{1/3}Co_{1/3}O_2$ was then added and the mixture was slightly heated (about 70 °C) while being stirred in order to evaporate the solvent. The resulting mixtures were heated at 400 °C for 5 h, and the $LiNi_{1/3}Mn_{1/3}Co_{1/3}O_2$ coated with the metal oxide was obtained. The amount of the coated metal oxide was ca. 3 wt%.

XRD measurements were carried out using a Rigaku Rint1000 diffractometer equipped with a monochromator and a Cu target tube.

A scanning electron microscope (SEM) study of the samples was performed using a Hitachi S-4000 electron microscope.

The surface properties of sample particles were investigated by X-ray photoelectron spectroscopy (XPS) using a JPS-9010 instrument.

The specific surface area for each sample was analyzed by the Brunauer, Emmett, and Teller (BET) method using Micromeritics Gemini2375 in which $N_2$ gas adsorption was employed. Each sample was heated to 120 °C for 1 h to remove adsorbed water before measurement.

A transmission electron microscope (TEM) observation was carried out using a JEM-2010 (JEOL) electron microscope.

The charge/discharge tests were carried out using a CR2032 coin-type cell, which consists of a cathode and lithium metal anode separated by a Celgard 2400 porous polypropylene film. The cathode contains a mixture of 3 mg of the accurately weighed active material and 2.2 mg of Teflonized acetylene black (TAB-2) as the conducting binder. The mixture was pressed onto a stainless steel mesh, whose geometric area was about 2 cm, and dried at 130 °C for 5 h. The cells were assembled in a glove box filled with dried argon gas. The electrolyte was 1 M $LiPF_6$ in ethylene carbonate/dimethyl carbonate (EC/DMC, 1:2, v/v). The cells after 100 cycles were disassembled in the glove box, and the cathodes were used as a working electrode in an electrochemical impedance spectroscopy (EIS) analysis after being washed three times with DMC.

The electrochemical impedance spectroscopy analysis was carried out using a home-made tri-electrode cell using metallic lithium as the counter and reference electrodes with 1 M $LiPF_6$ in ethylene carbonate/dimethyl carbonate (1:2, v/v) as the electrolyte. The geometric area of the working electrode was about 0.5 $cm^2$.

## 3. Results and discussion

Fig. 1 shows the XRD profiles of the bare $LiNi_{1/3}Mn_{1/3}Co_{1/3}O_2$ and $LiNi_{1/3}Mn_{1/3}Co_{1/3}O_2$ coated with the metal

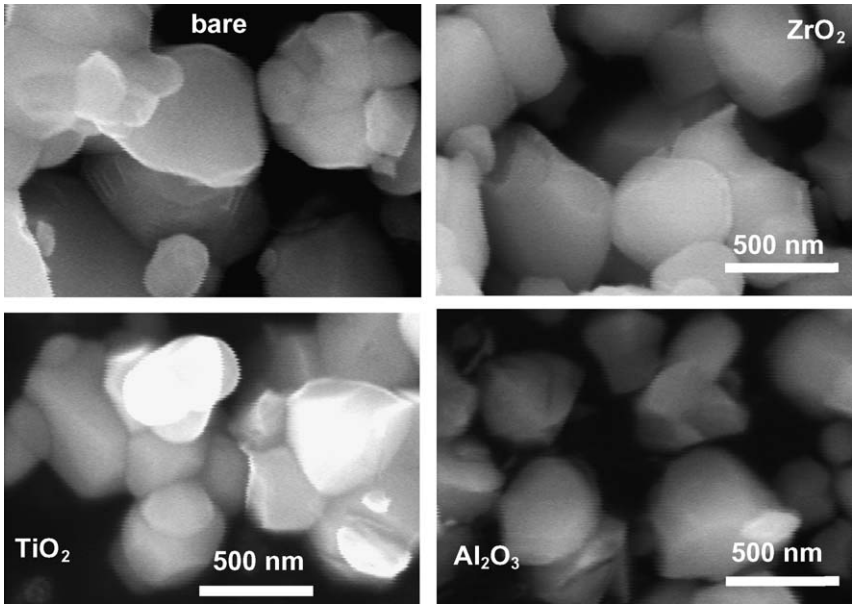


Fig. 2. SEM images of the $LiNi_{1/3}Mn_{1/3}Co_{1/3}O_2$ with and without the metal oxide coating.

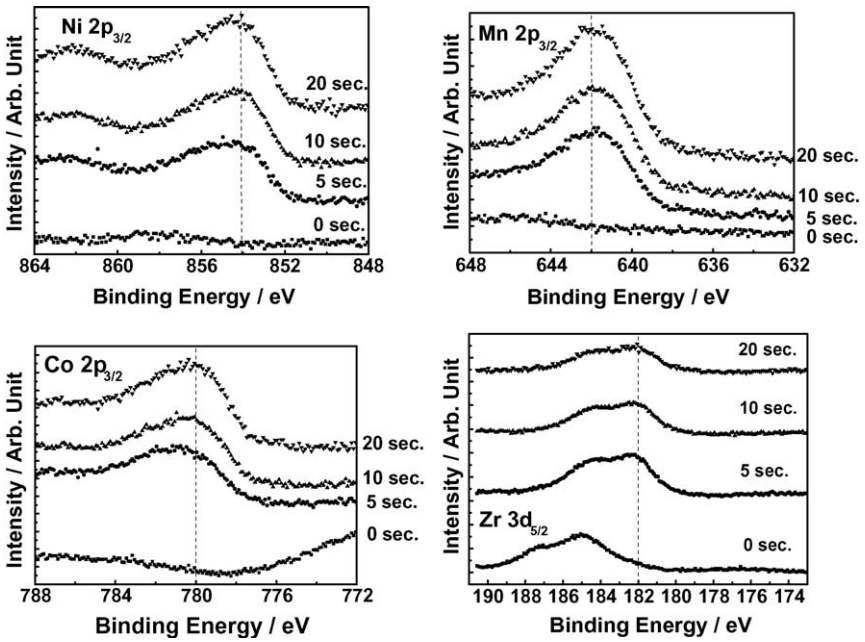


Fig. 3. Variation in the XPS emission spectra intensities in the $ZrO_2$-coated $LiNi_{1/3}Mn_{1/3}Co_{1/3}O_2$ with etching time.

oxides. All samples have a layered characteristic in terms of their XRD patterns, and all peaks could be indexed on the basis of the α-$NaFeO_2$ structure. The calculated lattice parameters of the bare $LiNi_{1/3}Mn_{1/3}Co_{1/3}O_2$ are 2.864 Å and 14.269 Å, consistent with the reported values [5]. The metal oxide addition shows no influence on the XRD patterns and no impurity diffractions or peak shifts were observed. These results suggest that there are no metal ions merged into the lattice and that these metal oxides should be amorphous.

SEM images of the $LiNi_{1/3}Mn_{1/3}Co_{1/3}O_2$ with and without the metal oxide coating are shown in Fig. 2. The particles of the bare $LiNi_{1/3}Mn_{1/3}Co_{1/3}O_2$ have an aggregated structure, consisting of well-shaped polyhedral primary particles, and the average size of the primary particles is on a nano-scale order. Due to the limits of both the relatively low coating content (3 wt% in this work) and the SEM resolution, the state of the metal oxides coating layer is difficult to be determined. Thus XPS analysis of the coated samples was carried out and the result is given in Fig. 3.

Fig. 3 demonstrates the variation in the XPS emission spectra intensities in the $ZrO_2$-coated $LiNi_{1/3}Mn_{1/3}Co_{1/3}O_2$ with etching time. Initially, the emission intensities of Ni, Mn, and Co were too weak to be detected. After being etched with Ar ions for 5 s, the signals of the transition metals appear, and their intensities are enhanced significantly with increased etching time. The binding energies of an electron in Ni $2p_{3/2}$, Mn $2p_{3/2}$, and Co $2p_{3/2}$ are 854.0, 642.0, and 780.0 eV, respectively. These values suggest that the valences of Ni, Mn, and Co in our sample are divalent, tetravalent, and trivalent, quite consistent with the reported values [18]. As for Zr $3d_{5/2}$, it consists of a broad main peak and a broad satellite peak centered at 185.0 and 187.0 eV, respectively. After being etched for 5 s, the peak positions shift to 182.0 and 184.0 eV, respectively. This result suggests that the valence of Zr is tetravalent. As the etching time increases, the binding energy is unaffected, while the peak intensity fades significantly. These results suggest that the $LiNi_{1/3}Mn_{1/3}Co_{1/3}O_2$ was coated with $ZrO_2$.

Fig. 4 shows the TEM image of the $ZrO_2$-coated $LiNi_{1/3}Mn_{1/3}Co_{1/3}O_2$. A thin $ZrO_2$ layer with a thickness of about 20 nm was observed on the particle surface of the

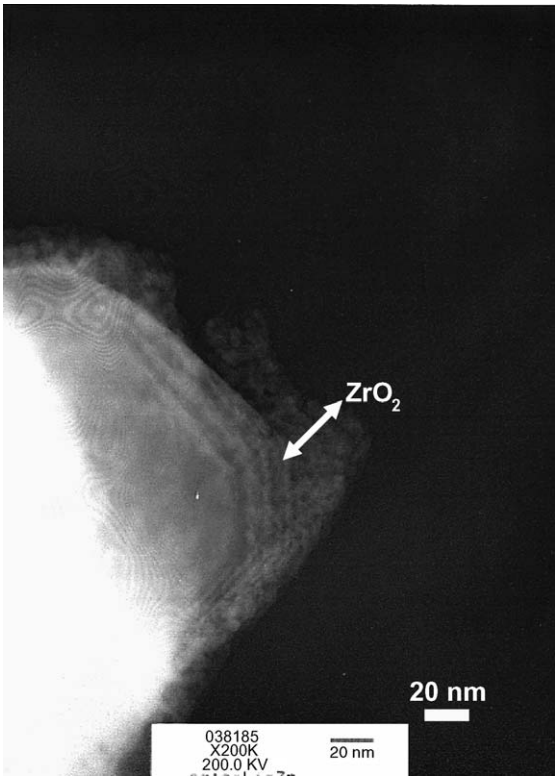


Fig. 4. TEM image of the $ZrO_2$-coated $LiNi_{1/3}Mn_{1/3}Co_{1/3}O_2$.

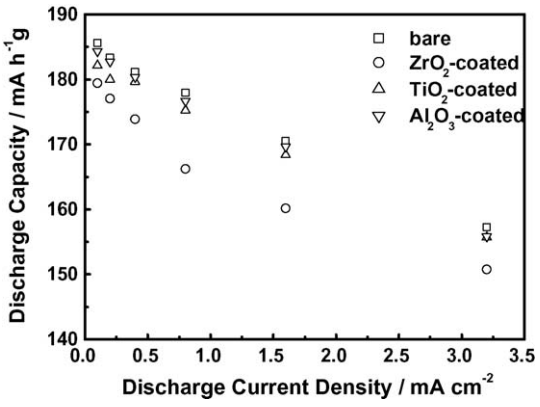


Fig. 5. Discharge capacities vs. discharge current densities of the $LiNi_{1/3}Mn_{1/3}Co_{1/3}O_2$ with and without the metal oxide coating.

$LiNi_{1/3}Mn_{1/3}Co_{1/3}O_2$. This thin layer is amorphous and porous. On the other hand, this thin layer is not continuous and its thickness is inhomogeneous. The specific surface area of the bare $LiNi_{1/3}Mn_{1/3}Co_{1/3}O_2$ is 2.01 $m^2\,g^{-1}$. The specific surface areas are 2.48, 2.44, and 2.43 $m^2\,g^{-1}$ for the samples coated with $ZrO_2$, $TiO_2$, and $Al_2O_3$, respectively. The increased specific surface area should originate from the metal oxide layer.

The discharge capacities versus discharge current densities of the $LiNi_{1/3}Mn_{1/3}Co_{1/3}O_2$ with and without the metal oxide coating are depicted in Fig. 5. All cells were charged at a constant current density of 0.1 mA $cm^{-2}$ (10 mA $g^{-1}$) in the range of 3–4.6 V. The bare $LiNi_{1/3}Mn_{1/3}Co_{1/3}O_2$ exhibits an excellent rate capability. When the discharge current density increases from 0.1 mA $cm^{-2}$ (10 mA $g^{-1}$) to 3.2 mA $cm^{-2}$ (320 mA $g^{-1}$) the discharge capacity decreases from 186 to 157 mAh $g^{-1}$; about 84% of the initial discharge capacity is retained. This result is quite consistent with the reported value [3,5]. The discharge capacities at a discharge current density of 0.1 mA $cm^{-2}$ (10 mA $g^{-1}$) of the samples coated with $ZrO_2$, $TiO_2$, and $Al_2O_3$ are 179, 182, and 184 mA h $g^{-1}$, respectively. When the discharge current density is 3.2 mA $cm^{-2}$ (320 mA $g^{-1}$), the discharge capacities are 151, 156, and 156 mA h $g^{-1}$ for the samples coated with $ZrO_2$, $TiO_2$, and $Al_2O_3$, respectively. These results suggest that the presence of the metal oxide layer slightly suppresses the rate capability, which is probably related to the low electronic conductivity of the metal oxide layer.

Fig. 6 shows the cyclic performances of the $LiNi_{1/3}Mn_{1/3}Co_{1/3}O_2$ with and without the metal oxide coating operated at 0.5*C* (about 110 mA $g^{-1}$) and 2*C* (about 420 mA $g^{-1}$). The initial charge/discharge capacities of the bare $LiNi_{1/3}Mn_{1/3}Co_{1/3}O_2$ operated at 0.5*C* are and 2*C* are 186/160 and 171/147 mA h $g^{-1}$, respectively. The irreversible capacities are 26 and 24 mA h $g^{-1}$, respectively. The initial charge/discharge capacities of the $ZrO_2$, $Al_2O_3$, and $TiO_2$ coated samples operated at 0.5*C* are 186/152, 187/154, and 182/148 mA h $g^{-1}$, respectively. The irreversible

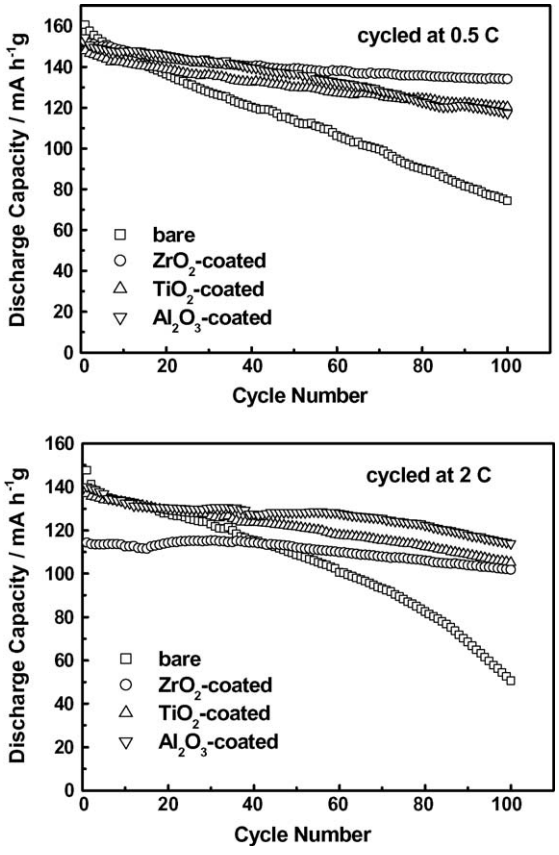


Fig. 6. Cyclic performances of the $LiNi_{1/3}Mn_{1/3}Co_{1/3}O_2$ with and without the metal oxide coating operated at 0.5*C* and 2*C* in 3–4.6 V.

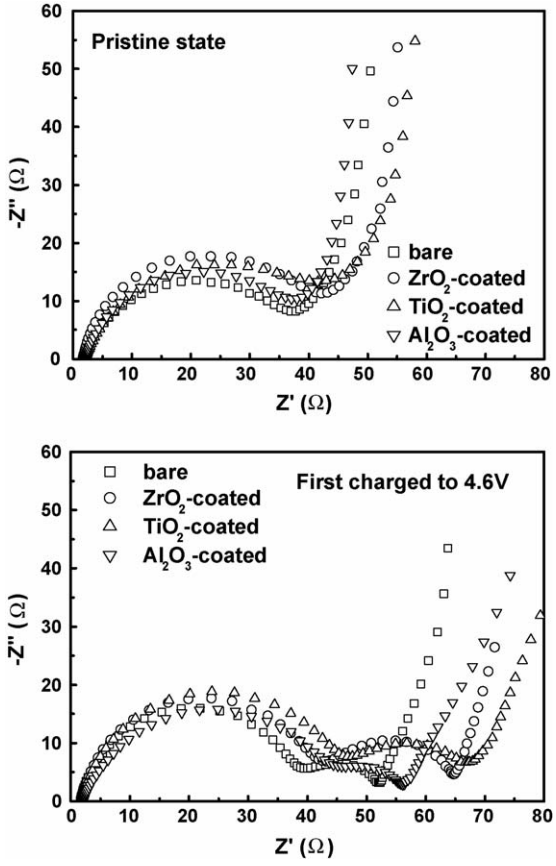


Fig. 7. Cole–Cole plots of the bare $LiNi_{1/3}Mn_{1/3}Co_{1/3}O_2$ and $LiNi_{1/3}Mn_{1/3}Co_{1/3}O_2$ coated with the metal oxides in the pristine state and when charged to 4.6 V.

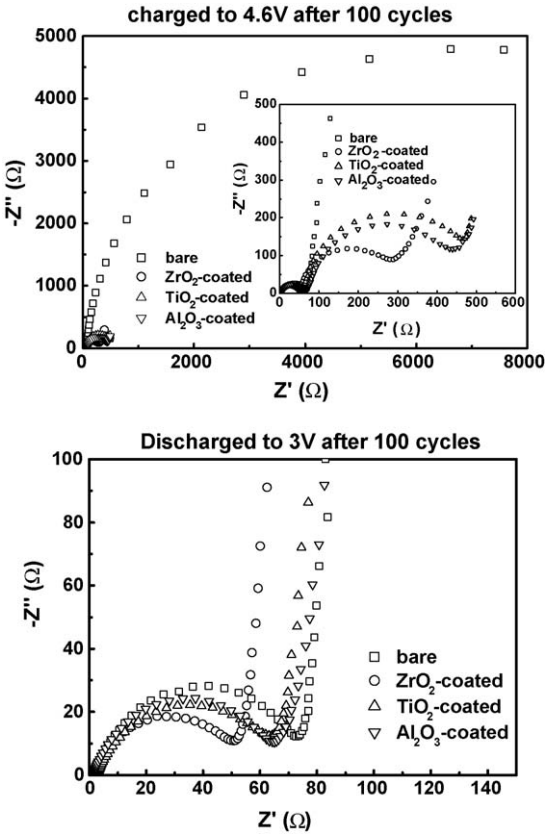


Fig. 8. Cole–Cole plots of the $LiNi_{1/3}Mn_{1/3}Co_{1/3}O_2$ with and without the metal oxide coating when charged to 4.6 V and at discharged to 3 V after 100 cycles operated at 0.5*C*.

capacities increase slightly to 34, 33, and 34 mA h $g^{-1}$ for $ZrO_2$, $Al_2O_3$, and $TiO_2$ coated samples compared to the bare $LiNi_{1/3}Mn_{1/3}Co_{1/3}O_2$, respectively. After 100 cycles, the discharge capacities of the bare $LiNi_{1/3}Mn_{1/3}Co_{1/3}O_2$ are 74 mA h $g^{-1}$ (at 0.5*C*, about 46% of the first discharge capacity) and 50 mA h $g^{-1}$ (at 2*C*, about 34% of the first discharge capacity), respectively. These results also confirmed that the cyclic performance of $LiNi_{1/3}Mn_{1/3}Co_{1/3}O_2$ depends on the operating current density as we previously reported [14]. All samples coated with the metal oxides exhibit improved cyclic performances compared to that of the bare $LiNi_{1/3}Mn_{1/3}Co_{1/3}O_2$ at both 0.5*C* and 2*C*, although the first discharge capacities slightly decrease. The discharge capacities of the samples coated with $ZrO_2$, $TiO_2$, and $Al_2O_3$ cycled at 0.5*C* after 100 cycles are 134, 120, and 117 mA h $g^{-1}$, which are about 88, 82, and 76% of the first discharge capacities, respectively. $LiNi_{1/3}Mn_{1/3}Co_{1/3}O_2$ coated with $ZrO_2$ shows the best capacity retention of all samples operated at both 0.5*C* and 2*C*.

In order to elucidate the change in electrochemical properties after the metal oxide coating, EIS analysis of the composite electrodes was carried out, and the results are shown in Figs. 7 and 8. Fig. 7 shows the Cole–Cole plots of the bare $LiNi_{1/3}Mn_{1/3}Co_{1/3}O_2$ and $LiNi_{1/3}Mn_{1/3}Co_{1/3}O_2$ coated with metal oxides in the pristine state and when charged to 4.6 V. A semicircle was observed for all samples in the high frequency domain, and its origin has been ascribed to the lithium ion migration through the interface between the surface layer of the particles and the electrolyte [19–21]. The calculated surface layer resistance and surface layer capacitance of the bare $LiNi_{1/3}Mn_{1/3}Co_{1/3}O_2$ are 38 Ω and 16.68 μF, respectively. As for the samples coated with metal oxides, the calculated surface layer resistance/surface layer capacitance are 43 Ω/36.67 μF, 38 Ω/42.32 μF, and 40 Ω/50.01 μF for $ZrO_2$, $TiO_2$, and $Al_2O_3$, respectively. These results suggest that the metal oxides coating layer has little influence on the surface layer resistance but significantly increases the surface layer capacitance, probably resulting from the increased specific surface area as mentioned above.

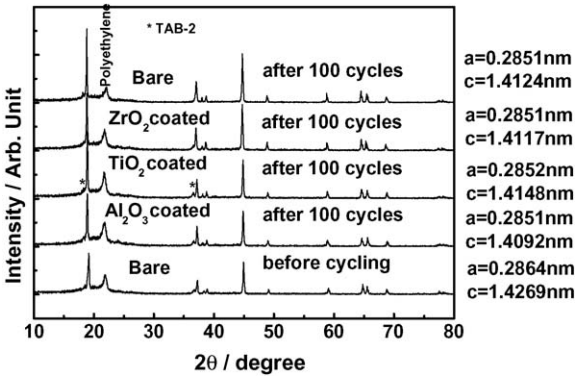


Fig. 9. Ex situ XRD of the metal oxide-coated $LiNi_{1/3}Mn_{1/3}Co_{1/3}O_2$ after 100 cycles operated at 0.5*C*.

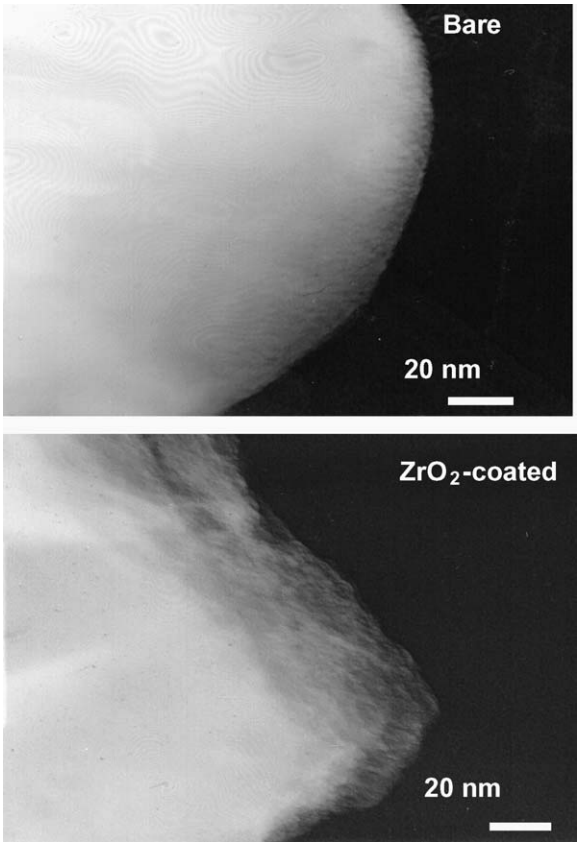


Fig. 10. TEM images of the bare $LiNi_{1/3}Mn_{1/3}Co_{1/3}O_2$ and $ZrO_2$-coated $LiNi_{1/3}Mn_{1/3}Co_{1/3}O_2$ after 100 cycles operated at 0.5*C*.

When the electrodes were charged to 4.6 V, no significant change was observed in this semicircle for all samples. However, a new depressed semicircle appears in the relatively low frequency region, whose origination could simply be assigned to the charge transfer resistance ($R_{ct}$). The bare $LiNi_{1/3}Mn_{1/3}Co_{1/3}O_2$ shows the smallest total resistance (sum of surface layer resistance and charge transfer resistance), which should be attributed to its best rate capability in this voltage range. The presence of the thin metal oxides layer slightly increases the charge transfer resistance ($R_{ct}$) and thereby increases the total resistance, quite consistent with the degradation in their rate capabilities.

Fig. 8 shows the Cole–Cole plots of the $LiNi_{1/3}Mn_{1/3}Co_{1/3}O_2$ with and without the metal oxide coating when charged to 4.6 V and discharged to 3 V after 100 cycles operated at 0.5*C*. As depicted in Fig. 7, the surface resistance of the bare $LiNi_{1/3}Mn_{1/3}Co_{1/3}O_2$ in both states increases to 80 Ω after 100 cycles, twice the initial value. We believe that it should be related to the change on the particle surface of the $LiNi_{1/3}Mn_{1/3}Co_{1/3}O_2$ during cycling. The presence of the metal oxides layer could effectively depress this change during cycling. $ZrO_2$-coated $LiNi_{1/3}Mn_{1/3}Co_{1/3}O_2$ exhibits an almost unchanged surface resistance after 100 cycles compared to its initial value. As for the charge transfer resistance ($R_{ct}$) at 4.6 V, it is about 13,000 Ω for the bare $LiNi_{1/3}Mn_{1/3}Co_{1/3}O_2$ after 100 cycles, far larger than its initial value (only about 10 Ω). Shaju et al. [22] had also observed the proportional increase in charge transfer resistance ($R_{ct}$) of the $LiNi_{1/3}Mn_{1/3}Co_{1/3}O_2$ with cycling when charged at 3.7 and 4.4 V. Although the increase in $R_{ct}$ was also observed in the samples coated with metal oxides, the total resistance of these samples is lower than 600 Ω after 100 cycles. These results suggest that the metal oxide coating on the surface of the $LiNi_{1/3}Mn_{1/3}Co_{1/3}O_2$ could effectively suppress the increase in the total resistance (especially in the charge transfer resistance) occurring during cycling. It should be noted that $ZrO_2$-coated $LiNi_{1/3}Mn_{1/3}Co_{1/3}O_2$ has an almost unchanged surface resistance as well as the smallest charge transfer resistance (smaller than 300 Ω) after 100 cycles, thereby showing the best cyclic performance in the range of 3–4.6 V.

It is well-known that charge transfer resistance involves many factors such as crystal structure, electronic conductivity, and the interparticle contacts (oxide–oxide, carbon–oxide, and carbon–carbon grain contacts) [23]. Therefore, we characterized the cycled electrodes by ex situ XRD, TEM, and SEM in order to elucidate the origin of the abnormal increase in the charge transfer resistance after long cycling.

Fig. 9 shows the ex situ XRD patterns of the bare $LiNi_{1/3}Mn_{1/3}Co_{1/3}O_2$ and the metal oxide-coated $LiNi_{1/3}Mn_{1/3}Co_{1/3}O_2$ after 100 cycles and their lattice parameters were indicated. All samples show reduced lattice volumes after 100 cycles compared to those at the pristine states, which should be attributed

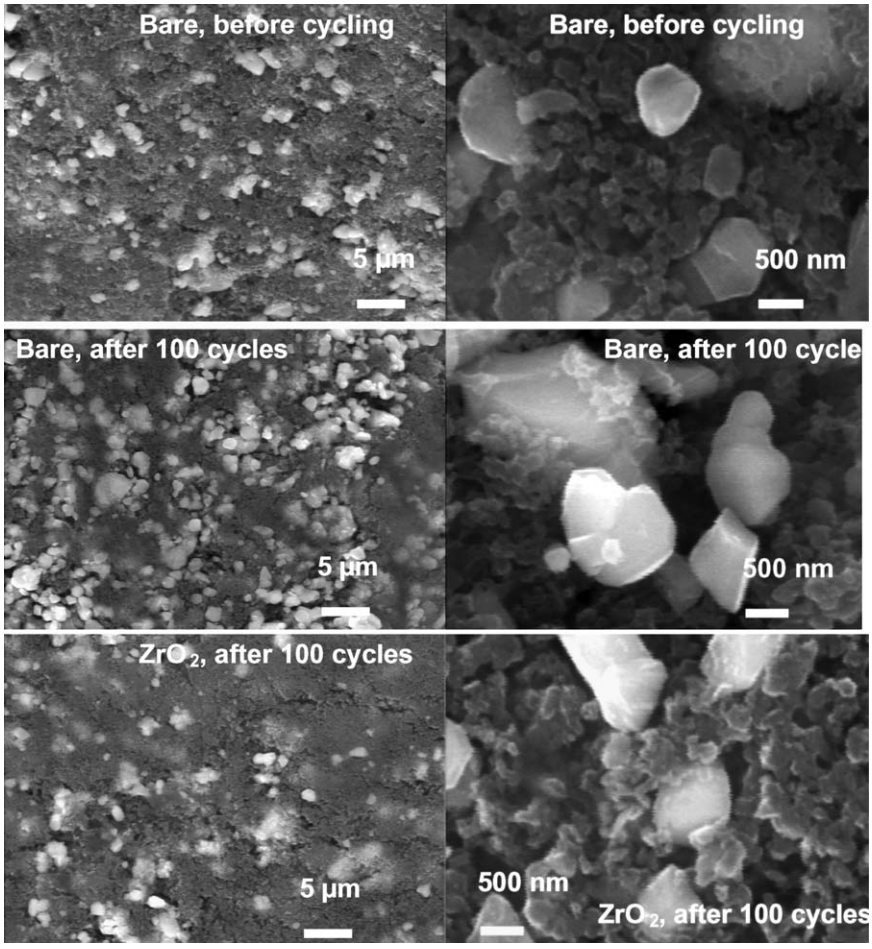


Fig. 11. Morphology evolution of the composite electrodes after 100 cycles operated at 0.5*C*.

to the reduced discharge capacities (in proportion to lithium content in the lattice). Nevertheless, no obvious change (new peaks appearing; phase transition, peak broadened . . .) was observed in all samples after 100 cycles compared to their pristine electrodes, implying that the structure of the $LiNi_{1/3}Mn_{1/3}Co_{1/3}O_2$ is stable during cycling.

TEM images of the bare $LiNi_{1/3}Mn_{1/3}Co_{1/3}O_2$ and $ZrO_2$-coated $LiNi_{1/3}Mn_{1/3}Co_{1/3}O_2$ after 100 cycles operated at 0.5*C* are depicted in Fig. 10. Both samples have no cracks or defects after 100 cycles. These results together with ex situ XRD analysis suggest that the abnormal increase in the charge transfer resistance of the $LiNi_{1/3}Mn_{1/3}Co_{1/3}O_2$ after long cycling is independent of the bulk degradation. It has been reported that the volume change in the $LiNi_{1/3}Mn_{1/3}Co_{1/3}O_2$ was very small when operated at 3–4.6 V [3,5]. Our results convince us that the structural exfoliation caused by volume variation is impossible in this voltage range. On the other hand, the surface of the bare $LiNi_{1/3}Mn_{1/3}Co_{1/3}O_2$ particle seems to become slightly coarse after 100 cycles, which is probably related to the increase in the surface resistance. In the case of the $ZrO_2$-coated $LiNi_{1/3}Mn_{1/3}Co_{1/3}O_2$, the coating layer is stable and no significant change was observed, quite consistent with the small change in its surface resistance after 100 cycles.

Fig. 11 shows the morphology change in the electrodes after 100 cycles. In the pristine electrode containing bare $LiNi_{1/3}Mn_{1/3}Co_{1/3}O_2$, the distribution of the $LiNi_{1/3}Mn_{1/3}Co_{1/3}O_2$ in TAB (binder/conductive agent) is generally homogeneous and the contact between the $LiNi_{1/3}Mn_{1/3}Co_{1/3}O_2$ particles and TAB is good. After being cycled for 100 cycles, the $LiNi_{1/3}Mn_{1/3}Co_{1/3}O_2$ particles seem to be self-aggregated, and their contact with TAB becomes poor due to the presence of many voids. In the case of the electrode containing the $ZrO_2$-coated $LiNi_{1/3}Mn_{1/3}Co_{1/3}O_2$, the active particles contact well with TAB and the morphology change is very small.

According to these results, we believed that the abnormal increase in the charge transfer resistance after long cycling should be the main reason for the capacity fading of the $LiNi_{1/3}Mn_{1/3}Co_{1/3}O_2$ operated in the range of 3–4.6 V. As for the mechanism of the abnormal increase in the charge transfer resistance after long cycling, we believe that it should not be originated from structural exfoliation because we could not observe the presence of a phase transition or cracks in the particles after 100 cycles. On the contrary, it should be ascribed to the change in both the particle surface and the morphologies of the $LiNi_{1/3}Mn_{1/3}Co_{1/3}O_2$ composite electrode after long cycling. As to the role of the metal oxide layer, we believed that its presence can not only effectively suppress the decomposition of the electrolyte solution on the charged particle surface, but also partially absorb the stress resulted from the volumetric change of the granules during the cycling, thereby reduce the strain of the binder/conductive agent and suppress the formation of the voids between the binder/conductive agent and active material particles.

## 4. Conclusions

In this work, we found that the $LiNi_{1/3}Mn_{1/3}Co_{1/3}O_2$ shows poor cyclic performances at 0.5*C* and 2*C* in the range of 3–4.6 V. The mechanism of the capacity fading was found to be related to the abnormal increase in the total resistance after long cycling. This abnormal increase in the total resistance has been attributed to the change in both the particle surface and the morphologies of the $LiNi_{1/3}Mn_{1/3}Co_{1/3}O_2$ composite electrode after long cycling. The presence of the metal oxide layer could effectively suppress the increase in the total resistance, thereafter improving the cyclic performance of the $LiNi_{1/3}Mn_{1/3}Co_{1/3}O_2$.

## Acknowledgement

This work was financially supported by the High-Tech Research Center Project for Private University: matching fund subsidy from the Ministry of Education, Culture, Sports, Science and Technology (MEXT) from 2001 to 2005.

## References

[1] T. Ohzuku, Y. Makimura, Chem. Lett. (2001) 642.
[2] K.M. Shaju, G.V. Subba Rao, B.V.R. Chowdari, Electrochim. Acta 48 (2002) 145.
[3] N. Yabuuchi, T. Ohzuku, J. Power Sources 119 (2003) 171.
[4] B.J. Hwang, Y.W. Tsai, D. Carlier, G. Ceder, Chem. Mater. 15 (2003) 3676.
[5] D. Li, T. Muta, L. Zhang, M. Yoshio, H. Noguchi, J. Power Sources 132 (2004) 150.
[6] J. Kim, H. Chung, Electrochim. Acta 49 (2004) 937.
[7] W. Yoon, C.P. Grey, M. Balasubramanian, X. Yang, D.A. Fischer, J. McBreen, Electrochem. Solid-State Lett. 7 (2004) A53.
[8] T. Cho, S. Park, M. Yoshio, Chem. Lett. 33 (2004) 704.
[9] Y.M. Todorov, K. Numata, Electrochim. Acta 50 (2004) 493.
[10] S. Myung, G. Kim, Y. Sun, Chem. Lett. 33 (2004) 1388.
[11] G. Kim, J. Kim, S. Myung, C. Yoon, Y. Sun, J. Electrochem. Soc. 152 (2005) A1707.
[12] J. Choi, A. Manthiram, J. Electrochem. Soc. 152 (2005) A1714.
[13] G.-H. Kim, S.-T. Myung, H.J. Bang, J. Prakash, Y.-K. Sun, Electrochem. Solid-State Lett. 7 (2004) A447.
[14] M. Kageyama, D. Li, K. Kobayakawa, Y. Sato, Y. Lee, J. Power Sources 157 (2006) 494–500.
[15] J. Cho, Y.J. Kim, T.J. Kim, B. Park, Angew. Chem. Int. Ed. Engl. 40 (2001) 3367.
[16] Z. Chen, J.R. Dahn, Electrochem. Solid-State Lett. 7 (2004) A11.
[17] Y. Lin, H. Wu, Y. Yen, Z. Guo, M. Yang, H. Chen, H. Sheu, N. Wu, J. Electrochem. Soc. 152 (2005) A1526.
[18] T.H. Cho, S.M. Park, M. Yoshio, T. Hirai, Y. Hideshima, J. Power Sources 142 (2005) 306.
[19] D. Aurbach, M. Levi, E. Levi, H. Teller, B. Markovsky, G. Salitra, U. Heider, L. Heider, J. Electrochem. Soc. 145 (1998) 3024.
[20] M. Levi, G. Salitra, B. Markovsky, H. Teller, D. Aurbach, U. Heider, L. Heider, J. Electrochem. Soc. 146 (1999) 1279.
[21] D. Aurbach, B. Markovsky, A. Rodkin, E. Levi, Y. Cohen, H. Kim, M. Schmidt, Electrochim. Acta 47 (2002) 4291.
[22] K.M. Shaju, G.V. Subba Rao, B.V.R. Chowdariz, J. Electrochem. Soc. 151 (2004) A1324.
[23] J. Fan, P.S. Fedkiw, J. Power Sources 72 (1998) 165.